

Improving SAT Solving with Graph Neural Networks

Wenxi Wang, Yang Hu, Mohit Tiwari, Sarfraz Khurshid, Kenneth McMillan, Risto Miikkulainen

The University of Texas at Austin

wenxiw@utexas.edu, huyang@utexas.edu, tiwari@austin.utexas.edu, khurshid@ece.utexas.edu, kenmcm@cs.utexas.edu, risto@cs.utexas.edu

Abstract

Propositional satisfiability (SAT) is an NP-complete problem that impacts many research fields, such as planning, verification, and security. Despite the remarkable success of modern SAT solvers, scalability still remains a challenge. Mainstream modern SAT solvers are based on the Conflict-Driven Clause Learning (CDCL) algorithm. Recent work aimed to enhance CDCL SAT solvers by improving its variable branching heuristics through predictions generated by Graph Neural Networks (GNNs). However, so far this approach either has not made solving more effective, or has required frequent online accesses to substantial GPU resources. Aiming to make GNN improvements practical, this paper proposes an approach called NeuroComb, which builds on two insights: (1) predictions of important variables and clauses can be combined with dynamic branching into a more effective hybrid branching strategy, and (2) it is sufficient to query the neural model *only once* for the predictions before the SAT solving starts. Implemented as an enhancement to the classic `MiniSat` solver, NeuroComb allowed it to solve 18.5% more problems on the recent SATCOMP-2020 competition problem set. NeuroComb is therefore a practical approach to improving SAT solving through modern machine learning.

Introduction

Propositional satisfiability (SAT) solvers are designed to check the satisfiability of a given propositional logic formula. SAT solvers have advanced significantly in recent years, which has fueled their applications in a wide range of domains. Despite this progress, scalability remains an issue. The solvers need to be both effective, i.e., solve more problems within a given time, and practical, i.e., not require excessive computational resources to do so.

Mainstream modern SAT solvers are based on the CDCL algorithm (Silva and Sakallah 2003). They often use a variable branching heuristic called Variable State Independent Decaying Sum (VSIDS; Moskewicz et al. 2001) to decide which variables are best to branch on at any given point. This paper aims to make CDCL SAT solvers more effective by using machine learning to improve VSIDS.

Recently, GNNs were proposed as a possible way to achieve this goal by training them to predict best branching variables. However, this approach has not usually made solvers more effective (Jaszczur, Łuszczuk, and Michalewski 2020; Kurin et al. 2019; Han 2020). One exception is

NeuroCore (Selsam and Bjørner 2019), which improved `MiniSat` (Eén and Sörensson 2003) by allowing it to solve 10% more problems on the SATCOMP-2018 (Heule et al. 2018) problem set. NeuroCore performs frequent online model inference to adjust its predictions with dynamic information extracted from the SAT solving process. This online inference is computationally demanding; their experiments required network access to 20 GPUs distributed over five machines. Such special requirement would be difficult to scale up to larger problems.

However, Selsam and Bjørner conjectured that a simple, hardcodeable heuristic might do just as well as the heuristic with the online neural predictions. Motivated by this idea, this paper proposes an approach called NeuroComb, which aims both to make solving more effective and to reduce the computational resource requirements, thus making the GNN approach more practical. This goal is achieved through two mechanisms: (1) learning to predict both which variables and which clauses are important, performing that inference only once before the solving process, and (2) applying the offline predictions repeatedly during the solving.

First, to obtain useful predictions, instead of focusing on only a single prediction task as NeuroCore does, NeuroComb makes two predictions: which variables are important (i.e., backbone variables and unsatisfiable core variables) and which clauses are important. By converting the input SAT formula into a compact graph representation, the problem of predicting important variables and clauses turns into two binary node classification problems. To get high-accuracy predictions for SAT formulas with diverse scales, NeuroComb employs a densely connected GNN architecture with pooling, both to ensure the model expressiveness and to avoid over-smoothing. To train the model with supervised learning, a dataset called DataComb containing 115,348 labeled CNF formulas with diversity was created by combining data from three different sources: Alloy (Jackson 2002), CNFgen (Lauria et al. 2017), and SATLIB (Hoos and Stützle 2000).

Second, the task of applying the predictions properly to SAT is accomplished in two steps: (1) information about important variables and clauses is extracted from the neural predictions before the solving begins, and (2) this information is applied *periodically* during the solving process, guiding the solver to possible good directions. This guidance is achieved by a hybrid branching heuristic that is based not only on the

original VSIDS dynamic information (the original dynamic heuristic), but also on the GNN-generated static information (the static heuristic).

NeuroComb is incorporated into `MiniSat` (Eén and Sörensson 2003), a classic CDCL SAT solver, to form a new solver called `NeuroComb-MiniSat`. The experimental results on all 400 SAT problems from the main track of SATCOMP-2020 (Balyo et al. 2020) show that NeuroComb makes `MiniSat` solve 18.5% more problems. All experiments were run on an ordinary commodity computer with one NVIDIA GeForce RTX 3080 GPU (10GB memory), one Intel Core i7-10700KF processor (16 logical cores), and 96GB RAM. The experiments thus demonstrate that NeuroComb is a practical approach to improve SAT solving through modern machine learning.

The DataComb dataset created for this work will be made publicly available upon acceptance of the paper; it should be a useful resource for other researchers aiming to utilize deep learning to enhance SAT solving in the future.

Background

This section introduces the SAT problem, CDCL algorithm, VSIDS heuristic, and basics of GNNs.

Preliminaries of SAT In SAT, a propositional logic formula ϕ is usually encoded in Conjunctive Normal Form (CNF), which is a conjunction (\wedge) of *clauses*. Each clause c is a disjunction (\vee) of *literals*. A literal l is either a variable v , or its complement $\neg v$. Each variable can be assigned a logical value, 1 (true) or 0 (false). A CNF formula has a satisfying assignment if and only if every clause has at least one true literal. For example, a CNF formula $\phi = (v_1 \vee \neg v_2) \wedge (v_2 \vee v_3)$ consists of two clauses $v_1 \vee \neg v_2$ and $v_2 \vee v_3$, four literals $v_1, \neg v_2, v_2$ and v_3 , and three variables v_1, v_2 , and v_3 . One satisfying assignment of ϕ is $v_1 = 1, v_2 = 1, v_3 = 0$. The goal of a SAT solver is to check if a formula ϕ is satisfiable (sat) or unsatisfiable (unsat). A *complete* solver either outputs a satisfying assignment for ϕ , or proves that no such assignment exists. In the unsat case, many solvers can produce a subset of the clauses that is unsat, called an *unsat core*.

CDCL Algorithm CDCL makes SAT solvers efficient in practice and is one of the main reasons for the widespread of SAT applications. The general idea of CDCL algorithm is as follows (see Marques-Silva, Lynce, and Malik 2021 for details). First, it picks a variable on which to branch with the branching heuristic and decides a value to assign to it. It then conducts a Boolean propagation based on the decision. In the propagation, if a conflict occurs (i.e., at least one clause is mapped to 0), it performs a conflict analysis; otherwise, it makes a new decision on another selected variable. In the conflict analysis, CDCL first analyzes the decisions and propagations to investigate the reason of the conflict, then extracts the most relevant wrong decisions, undoes them, and adds the reason to its memory as a learned lesson (encoded in a clause called *learned clause*) in order to avoid making the same mistake in the future. The above steps of clause learning in conflict analysis are called *resolution steps*. Since the memory space is limited, it forgets older learned clauses when necessary and keeps newer ones learned from more recent

conflicts. The process continues until all the variables are assigned a value and no conflicts occur (in case the problem is sat), or until it learns the empty clause, or "false" (in case the problem is unsat).

The VSIDS Branching Heuristic The VSIDS heuristic (Moskewicz et al. 2001) is the dominant branching heuristic in CDCL SAT solvers. Many high-performance branching heuristics are variants of VSIDS. The essence of VSIDS is an *additive bumping* and *multiplicative decay* behavior. VSIDS maintains an *activity score* for each variable in the Boolean formula. The score is typically initialized to 0 at the first run of a solver. If a variable is involved in a resolution step of the conflict analysis, its activity score is additively bumped by a fixed increment. After every conflict analysis, regardless of the involvements, the activity score of every variable is decayed multiplicatively by a constant factor γ : $0 < \gamma < 1$. VSIDS selects the variable with the highest score on which to branch. The idea is to favor variables that participate in more recent conflict analyses.

Message Passing in GNN GNNs (Wu et al. 2020; Zhou et al. 2020) are a family of neural network architectures that operate on graphs (Gori, Monfardini, and Scarselli 2005; Scarselli et al. 2008; Gilmer et al. 2017; Battaglia et al. 2018). Typical GNNs follow a recursive neighborhood aggregation scheme called message passing (Gilmer et al. 2017).

Formally, the input of a GNN is a graph defined as a tuple $G = (V, E, W, H)$, where V denotes the set of nodes; $E \subseteq V \times V$ denotes the set of edges; $W = \{W_{u,v} | (u, v) \in E\}$ contains the feature vector $W_{u,v}$ of each edge (u, v) ; and $H = \{H_v | v \in V\}$ contains the feature vector H_v of each node v . A GNN maps each node to a vector-space embedding by updating the feature vector of the node iteratively based on its neighbors. For each iteration, a message passing layer \mathcal{L} takes a graph $G = (V, E, W, H)$ as input and outputs a graph $G' = (V, E, W, H')$ with updated node feature vectors, i.e., $G' = \mathcal{L}(G)$. Classic GNN models (Gilmer et al. 2017; Kipf and Welling 2016) usually stack several message passing layers to realize iterative updating.

Each message passing layer consists of two operations: message generation and message aggregation. For each edge $(x, y) \in E$, a message $M_{x,y}$ is generated via function \mathcal{R} :

$$M_{x,y} = \mathcal{R}(W_{x,y}, H_x, H_y). \quad (1)$$

For each node y , messages from all neighbors of y (denoted as N_y) are aggregated via function \mathcal{Q} as

$$H'_y = \mathcal{Q}(H_y, \{M_{x,y} | x \in N_y\}). \quad (2)$$

Prior work on utilizing GNNs to improve CDCL SAT solving will be reviewed next.

Related Work

Several approaches have recently been developed to utilize GNNs to facilitate CDCL SAT solving. NeuroSAT (Selsam et al. 2018) was the first such framework adapting a neural model into an end-to-end SAT solver, which was not intended as a complete SAT solver. Other applications aim to provide SAT solvers with better heuristics, including in particular the

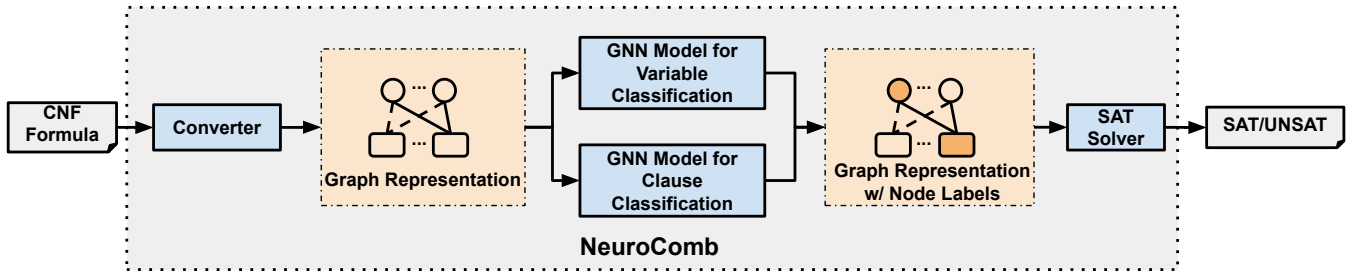


Figure 1: Overview of NeuroComb. First, the input CNF formula is converted into a compact graph representation. Two trained GNN models are then applied once on the graph before SAT solving begins: one model classifies the variables in the graph and the other classifies the clauses. The SAT solver utilizes the resulting labeled graph periodically to inform its solving process. Thus, with the offline process of creating informative labels and the online process of utilizing them properly, NeuroComb makes the solving more effective and practical.

branching heuristic. Jaszczur, Łuszczuk, and Michalewski (2020) used an architecture similar to NeuroSAT to enhance the branching heuristic in both DPLL (Davis, Logemann, and Loveland 1962) and CDCL algorithms. Kurin et al. (2019) proposed a branching heuristic called GQSAT trained with value-based reinforcement learning. In NeuroGlue, Han (2020) trained a network to predict glue variables, i.e. those likely to occur in glue clauses, which are conflict clauses identified by the Glucose series of solvers (Audemard and Simon 2018). Although these approaches reduce the number of solving iterations, they do not provide obvious improvements in solving effectiveness.

In contrast, NeuroCore (Selsam and Bjørner 2019), the most closely related approach to this paper, aims to make the actual solving more effective. It enhances VSIDS branching heuristic for CDCL using supervised learning to map unsat problems to unsat core variables (i.e., the variables involved in the unsat core). Selsam and Bjørner are aware of the fact that perfect predictions of the unsat core do not always yield a useful branching heuristic. In some problems, the smallest core may include every variable, and in sat problems, there are no cores at all. Therefore, NeuroCore relies on *imperfect* prediction, with the hope that the variables assigned with higher probability correlate well with the variables that form a good basis for branching. Based on the dynamically learned clauses during the solving process, NeuroCore performs frequent online model inference to tune the predictions. This online inference is computationally demanding, requiring 20 GPUs evenly distributed over five machines in their experiments. The main idea of NeuroComb is to utilize more informative offline predictions and apply them efficiently enough to make the approach practical.

NeuroComb

In order to reduce the computational cost of the online model inference and to make SAT solving more effective, NeuroComb utilizes static high-quality model predictions. Instead of focusing on only one term (e.g., unsat core variables), NeuroComb integrates information on the predictions of three terms (i.e. two important variable terms and one important clause term), thus improving reliability. The model inference is performed only once before the SAT solving process, and the resulting offline predictions is applied periodically during

the solving. Fig. 1 shows the overview of NeuroComb. Its components are described in detail in the subsections below.

Graph Representation of CNF formulas

As in recent work (Kurin et al. 2020; Yolcu and Póczos 2019), a SAT formula is represented using a more compact undirected bipartite graph than the one adopted in NeuroCore. Two node types represent the variables and clauses, respectively, and two edge types represent two polarities, i.e. the variable itself and its complement. Formally, for a graph representation $G = (V, E, W, H)$ of a SAT formula, the edge feature $W_{u,v}$ of each edge (u, v) is initialized by its edge type with the value 1 representing positive polarity and -1 negative polarity; the node feature H_v of each node v is initialized by its node type with 0 representing a variable and 1 a clause.

Classifying Variables and Clauses

Important Variables We identify two types of important variables in SAT: *unsat core variables* for unsat problems as NeuroCore, and *backbone variables* for sat problems. The unsat core variables are important because they occur in the proof of unsatisfiability. Backbone variables (Parkes 1997) refer to variables that have the same value in every satisfying assignment. Note that backbone variables are seldom considered to improve the efficiency of modern SAT solvers, because computing the backbone variables is hard in general (Previti and Jarvisalo 2018; Janota, Lynce, and Marques-Silva 2015; Kilby et al. 2005). However, if backbone variables can be efficiently estimated, they can be helpful in reducing the search space and thus facilitating SAT solving.

Important Clauses An important insight in NeuroComb is that clauses involved in more resolution steps in conflict analysis are more important. Consequently, an importance score s_c of the clause c can be defined as $s_c = k_c/K$, where K denotes the total number of resolution steps in the entire SAT solving and k_c denotes the number of times that clause c participates in resolution steps. In contrast to the activity score with decay in CDCL SAT solvers, which indicates how actively a variable participates *locally* in recent conflict analyses, this importance score indicates how often the clause participates *globally* in conflict analyses during the entire SAT solving process. Clauses with an importance

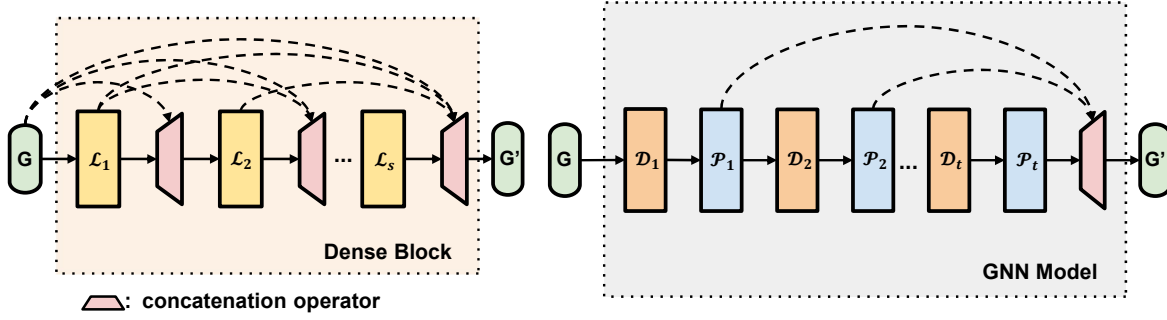


Figure 2: The architecture of the GNN model in NeuroComb. Labels $\mathcal{L}_1, \dots, \mathcal{L}_s$ refer to message-passing layers, $\mathcal{D}_1, \dots, \mathcal{D}_t$ to dense blocks, and $\mathcal{P}_1, \dots, \mathcal{P}_t$ to pooling layers.

score higher than a threshold θ are deemed important. In the current implementation, θ is set to 0, giving a loose definition for the important clauses: any clauses participating at least once in the resolution steps are taken as important.

Classification Classifying important variables and clauses is taken as two binary node classification tasks. Two GNN models with the same architecture are trained with the same loss function type called Binary cross entropy (BCE) but targeting the corresponding node types. Given a graph G representing an input CNF formula, each GNN model outputs a graph G' with updated node feature vectors, which are then fed to a multi-layer perceptron model for node classification.

The GNN Model Architecture of NeuroComb

In this subsection, the architecture of the GNN model is introduced including three key components: message passing, dense blocks, and pooling.

Message Passing As introduced in Equation 1 and Equation 2, each message-passing layer \mathcal{L} consists of two operations: message generation via function \mathcal{R} and message aggregation via function \mathcal{Q} . In NeuroComb, function \mathcal{R} is realized with a multi-layer perceptron model \mathcal{M}_1 :

$$\mathcal{R}(W_{x,y}, H_x, H_y) = \mathcal{M}_1(W_{x,y} \cdot (H_x \parallel H_y)), \quad (3)$$

where \parallel denotes vector concatenation. Function \mathcal{Q} is realized based on messages from all neighbors N_y as

$$\mathcal{Q}(H_y, \{M_{x,y} | x \in N_y\}) = \mathcal{A}(\mathcal{B}(\mathcal{M}_2(H_y) + \sum_{x \in N_y} M_{x,y})), \quad (4)$$

where \mathcal{A} denotes the activation function, \mathcal{B} denotes batch normalization (Santurkar et al. 2018), \mathcal{M}_2 denotes another multi-layer perceptron model: one that transforms H_y into an intermediate representation with the same dimensions as the messages.

Dense Blocks Inspired by the design of Graph Convolutional Networks (Kipf and Welling 2016), multiple message passing layers are stacked in NeuroComb to make the model more expressive. One key hyperparameter is *model depth*, i.e., the number of message-passing layers. In order to let the messages pass sufficiently through the graph and thus enable each node to learn the whole graph structure, model depth is usually set to at least the diameter of the input graph (Loukas

2019). However, due to the diverse CNF formula scales, corresponding graph representations have various diameters, which makes it difficult to determine what an ideal model depth is for all potential graph inputs. Deeper models usually lead to *over-smoothing* (Li, Han, and Wu 2018) when applied to smaller graphs, while shallower models may not be sufficiently expressive when applied to larger graphs.

In NeuroComb, a sufficiently deep model is used to make sure it is expressive enough, and *dense connectivity* is used to overcome over-smoothing. Inspired by DenseNet (Huang et al. 2017) and DeepGCN (Li et al. 2019), a *dense block* is constructed by stacking and connecting the message-passing layers in a dense manner, as shown in Fig. 2 (left). Each message-passing layer obtains its inputs by concatenating the outputs from all its preceding message-passing layers. Formally, a dense block is recursively defined as

$$\mathcal{D}^{(s)}(G) = \begin{cases} \mathcal{L}_s(\mathcal{D}^{(s-1)}(G)) \parallel \mathcal{D}^{(s-1)}(G), & s > 0 \\ G, & s = 0, \end{cases} \quad (5)$$

where s denotes the number of message-passing layers, \mathcal{L}_s denotes s -th message passing layer, \parallel is the graph concatenation operator satisfying $(V, E, W, H) \parallel (V, E, W, H') = (V, E, W, \{H_y \parallel_h H'_y | y \in V\})$, and \parallel_h denotes the vector concatenation operator.

Pooling With dense blocks, a deep and expressive GNN model can be built. One straightforward way is to construct it as one deep dense block. However, this approach tends to produce *high-dimensional* node feature vectors. Such vectors would reduce the performance of the node classifier because of the curse of dimensionality (Wojtowysch and E 2020). To address this problem, *shallow* dense blocks are stacked and one pooling layer is added to the end of each block to reduce the dimension of the block output, as shown in the right side of Fig. 2. Instead of concatenating the outputs directly from all dense blocks, NeuroComb concatenates the outputs of all pooling layers as the final node feature vectors. Formally, a GNN model with pooling is defined as

$$\mathcal{J}^{(t)}(G) = \parallel_{i=1}^t \mathcal{P}_i(\mathcal{D}_i^{(s)}(\dots \mathcal{P}_1(\mathcal{D}_1^{(s)}(G))), \quad (6)$$

where t denotes the number of dense blocks, \parallel the graph concatenation operator, \mathcal{P}_i the i -th pooling layer, and $\mathcal{D}_i^{(s)}$ the i -th dense block, which consists of s message-passing layers. Since using the common local pooling layers could be

less helpful in improving the GNN performance (as shown in the recent work of Mesquita, Souza, and Kaski 2020), the message-passing layer, which outputs lower dimensional node feature vectors, is utilized as the pooling layer.

Implementation The current implementation of the GNN model consists of two dense blocks with three message-passing layers each ($s = 3, t = 2$). The multi-layer perceptron of each message-passing layer has two hidden layers with the dropout rate of 0.25. The activation function is Exponential Linear Unit (ELU; Clevert, Unterthiner, and Hochreiter 2015). The model is implemented using PyTorch (Paszke et al. 2019) and PyTorch Geometric (Fey and Lenssen 2019).

Training The two GNN models for the classification tasks were trained on our entire DataComb dataset, using the AdamW optimizer (Loshchilov and Hutter 2017) with an initial learning rate of 10^{-3} and a weight decay coefficient of 10^{-2} . The batch size was set to eight and the number of epochs to 20 for each training run. The training for both tasks took 14 hours in total on the commodity computer.

Applying GNN Predictions in SAT

The goal is to utilize the important variable and clause predictions from the GNN models to improve the VSIDS variable branching heuristic of CDCL solvers. The predictions are used as static information characterizing the SAT problem. The insight is to utilize such static information effectively to guide the dynamic VSIDS variable branching heuristic.

Extracting Static Information The first step is to extract the static information from the GNN predictions. The idea is to make the final static scores robust to prediction errors by combining the important variable prediction with the important clause prediction. Higher scores are assigned to variables that are important (i.e., unsat core variables or backbone variables) and also appear more frequently in important clauses. Formally, the static score s_v of the variable v is defined as

$$s_v = \alpha p_v + (1 - \alpha) \mathcal{N} \left(\sum_{c \in C_v} p_c \right), \quad (7)$$

where $p_v \in [0, 1]$ denotes the important variable prediction score of variable v ; $p_c \in [0, 1]$ denotes the important clause prediction score of clause c ; C_v denotes the set of all clauses containing variable v ; $\alpha \in (0, 1)$ is a hyperparameter for the weighted mean between two prediction scores. Further, \mathcal{N} denotes the function that normalizes the accumulated prediction score $q_v = \sum_{c \in C_v} p_c$ to the range $[0, 1]$:

$$\mathcal{N}(q_v) = \frac{q_v - \min_{u \in U}(q_u)}{\max_{u \in U}(q_u) - \min_{u \in U}(q_u)}, \quad (8)$$

where U denotes the set of all variables in a SAT formula.

Applying Static Information Next, the static information needs to be utilized to enhance the VSIDS branching heuristic. A hybrid branching heuristic is proposed to branch on variables not only based on their VSIDS activity scores (referred to as *dynamic branching*) but also based on their static scores (referred to as *static branching*, i.e., branching on the undecided variable with the highest static score). Dynamic

branching remains the primary branching strategy but is interrupted periodically (with a period denoted by β) by static branching that lasts only a short time at each turn (with a duration denoted as γ). This hybrid strategy aims to guide the solver periodically to possible good directions by drawing attention to the important variables indicated by the static scores. The insight is that small and periodic perturbations produced by the static branching should not only change a number of branching decisions, but also slowly and profoundly influence the solver states because the new decisions that lead to conflicts affect the future VSIDS scores.

The interruption and time-limited effect of static branching is inspired by the dynamic inference in NeuroCore. However, this mechanism could make the solving process non-deterministic because SAT solvers conduct thousands of searches per second and the solver status could change even within a microsecond, and there is no such accurate timing mechanism providing the guarantee. To make sure that the process remains deterministic, the interrupt period β is quantified with the number of conflicts (denoted as β_f), by estimating the frequency of conflict generation (denoted as m_f) measured in conflicts per second:

$$\beta_f = \beta m_f. \quad (9)$$

Similarly, the effect duration γ is quantified with the number of branching decisions (denoted as γ_d), by estimating the frequency of decision generation (denoted as m_d) measured in decisions per second. Since the decision frequency can be estimated with the conflict frequency using the ratio of the number of decisions to the number of conflicts (denoted as n), the quantification of the effect duration γ is

$$\gamma_d = \gamma m_d = \gamma n m_f. \quad (10)$$

The key of realizing the transformations in Equation 9 and Equation 10 lies in estimating the conflict frequency m_f . Since m_f is changing over time, it is estimated dynamically based on the solver status. This is a regression problem and can be solved e.g., by the Random Forest machine learning method (Liaw, Wiener et al. 2002), trained to predict conflict frequency based on features that describe the current solver status. These features include the number of undecided variables, the number of not yet satisfied original clauses, the number of literals in these clauses, the number of learned clauses, the average number of literals in each learned clause, the number of literals in conflict clauses, the number of decisions, and the number of propagations. To generate data, the selected SAT solver, MiniSat, was run on 1,200 SAT formulas randomly selected from DataComb with a timeout of 100 seconds, collecting data every 10 seconds. The mean squared error is applied as the loss function. The average R^2 score of the ten-fold cross validation on all generated 11,502 samples is 0.991 (± 0.002). The final conflict frequency predictor is obtained by training the model on all samples.

The detailed algorithm of the hybrid branching approach is illustrated in the appendix.

Implementation The classic MiniSat solver was adapted to support the hybrid branching strategy. The implementation is called NeuroComb-MiniSat. For hyperparameter tuning, α was tried with 0.3, 0.4, 0.5, 0.6, and 0.7;

Table 1: Details of the Source and Combined Datasets

Dataset	Alloy			CNFgen			SATLIB			DataComb		
# cnf	58,201			34,483			41,526			115,348		
Stats	min	max	avg	min	max	avg	min	max	avg	min	max	avg
# var	829	41,674	11,482	5	32,766	1,886	48	6,325	114	5	41,647	4,470
# cla	1,170	68,207	19,209	15	105,116	5,363	50	134,621	517	15	134,621	8,290

β with 90, 120, and 150 seconds; γ with 1000^{-1} , 900^{-1} , and 800^{-1} seconds. Based on the average solving time on 100 selected hard problems from DataComb, α was set to 0.5, β to 150 seconds, and γ to 800^{-1} seconds (1.25 milliseconds).

Dataset

Training Dataset A new dataset containing CNF formulas with labeled important variables and clauses, called DataComb, was created for training our GNN model. The CNF formulas are obtained using three sources: a software modeling tool called Alloy (Jackson 2002), a recent CNF generator called CNFgen (Lauria et al. 2017), and an online dataset called SATLIB benchmark library (Hoos and Stützle 2000). Important variables are labeled in each CNF formula using two publicly available tools: MiniBones (Previti and Jarvisalo 2018) to provide the backbone variables, and Kissat (the winner of the SATCOMP-2020; Fleury and Heisinger 2020), to provide the unsat core variables. Important clauses are labeled based on the clause importance score provided by MiniSat. The timeout for generating the CNF formulas is 60 seconds and for getting the labels is 200 seconds.

Table 1 shows the details of the resulting dataset. Alloy is a mature toolset that models real-world problems from a wide range of applications and translates them into CNF formulas. As a base, 119 problems were first selected, ranging from security in protocols and type checking in programming languages to media asset management and network topology. Alloy models typically have scale parameters, such as the number of processes in a protocol, allowing us to generate problems of varying size. The sizes of 119 problems were then varied systematically, generating a total of 58,201 CNF formulas (with labels). CNFgen complements Alloy well in that it instead generates CNF formulas that appear in proof complexity literature. CNFgen generated 34,483 CNF formulas (with labels), grouped by six categories: pigeon-hole principle, subset cardinality, counting principle, pebbling game, random k-CNF, and clique-coloring. SATLIB, on the other hand, is a library of known benchmark instances and therefore provides a baseline challenge. From SATLIB, 41,526 CNF formulas (with labels) were included, encoding four kinds of combinatorial problems: random-3-SAT, graph coloring, planning, and all-interval series (AIS)¹. Altogether from these three sources, 134,210 labeled CNF formulas were obtained, consisting of 57,674 sat and 76,536 unsat formulas. To make the dataset balanced, 57,674 unsat formulas were randomly selected from the initial set, for a final DataComb dataset of 115,348 labeled CNF formulas.

In Table 1, the number of variables and the number of clauses are used to characterize the size of the CNF formulas.

¹For details about AIS problem, please refer to the link: <https://www.cs.ubc.ca/~hoos/SATLIB/Benchmarks/SAT/AIS/descr.html>

The formulas generated by Alloy are generally larger than those generated by CNFgen, which are in turn larger than those originating from SATLIB. DataComb thus contains a diverse set of formulas: the number of variables ranges from five to 41,647, with an average of 4,470; the number of clauses ranges from 15 to 134,621, with an average of 8,290.

Testing Dataset To evaluate the effectiveness of NeuroComb-MiniSat, we choose all 400 CNF formulas from the main track of SATCOMP-2020 (Balyo et al. 2020) as the testing data. Note that the testing dataset is not only an unseen set, but also completely independent from the training set, DataComb, whose generation does not consider any of the problems from previous SAT competitions (in contrast with e.g., NeuroCore experiments, where part of the training set was generated based on problems from SATCOMP-2017, and the testing set was from SATCOMP-2018). In particular, the average number of variables per formula is 69 times larger, and the average number of clauses 483 times larger, in the testing set than in the training set.

Experiments

The experiments aim to answer three research questions:

RQ1: *How accurately does the GNN model identify important variables and clauses?*

RQ2: *How effective is NeuroComb-MiniSat compared to MiniSat?*

RQ3: *How much do the predictions and the hybrid way of applying the predictions each contribute to the performance of NeuroComb-MiniSat?*

Table 2: Performance of the GNN model in Classifying Important Variables and Clauses

Task	Stats	Precision	Recall	F_1	Accuracy
Variable		0.941 \pm 0.015	0.778 \pm 0.014	0.852 \pm 0.005	0.902 \pm 0.003
Clause		0.929 \pm 0.005	0.820 \pm 0.008	0.871 \pm 0.003	0.937 \pm 0.001

RQ1: GNN Model Performance The GNN model was evaluated with the ten-fold cross validation on DataComb. Table 2 shows the average (\pm stdev) prediction performance for both tasks in terms of precision, recall, F_1 score and accuracy. The model is able to classify 90.2% of the variables and 93.7% of the clauses correctly, both with over 90% precision and over 0.85 F_1 score. Therefore, *the GNN model learns to classify both important variables and important clauses well.*

RQ2: NeuroComb Performance To evaluate the solving effectiveness, NeuroComb-MiniSat and MiniSat were applied to all 400 testing SAT problems in the testing dataset, with the standard time out of 5,000 seconds. Each solver utilized up to 16 different processes in parallel on the dedicated 16-core machine. The solving time of

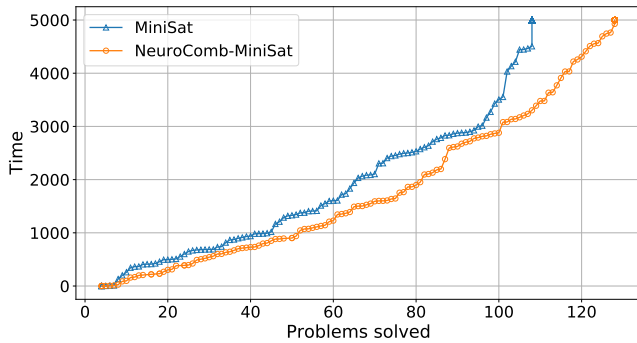


Figure 3: Progress of NeuroComb-MiniSat and MiniSat over time in solving the 400 test problems (time in seconds). NeuroComb-MiniSat takes the lead early on, and the difference becomes more pronounced as the instances take longer to solve.

NeuroComb-MiniSat includes both the model inference time and the SAT solving time. The static information extraction time is negligible.

The inference was run on the GPU for those 302 problems that fit into GPU memory and on a CPU for those 92 problems that do not fit into GPU memory but fit into RAM. No inference was run for the remaining 6 problems, thus reducing NeuroComb-MiniSat to MiniSat in those cases. The total time of the GPU inference ranged from 0.005 to 0.41 sec, with an average of 0.01 sec, and the CPU inference from 39.0 to 656.2 sec, with an average of 218.9 sec.

In terms of effectiveness, NeuroComb-MiniSat solved 128 problems, whereas MiniSat only solved 108, which amounts to an improvement of 18.5%. Most of the improvement comes from solving more sat problems: NeuroComb-MiniSat solved 70 of them while MiniSat solved only 55, an increase of 27%. On the other hand, NeuroComb-MiniSat solved only 5% more unsat problems (55 vs. 58). Fig. 3 shows the progress of the two solvers over time. NeuroComb-MiniSat takes the lead after the first few minutes, increases it substantially at 3,000 seconds, and maintains the lead until the end. Fig. 4 shows a scatter plot of the solving time for each problem. There are many problems that can be solved by NeuroComb-MiniSat under 1,000 seconds that MiniSat cannot solve in 5,000 seconds; the opposite rarely happens. Overall, the results show that NeuroComb-MiniSat *is more effective than MiniSat* on the SATCOMP-2020 problems.

RQ3: Contributions of the predictions vs. the application

To understand where NeuroComb-MiniSat’s power comes from, an ablation method called Random-MiniSat was created. This method is otherwise identical to NeuroComb-MiniSat but obtains its static information from uniformly random variable and clause prediction scores within $[0, 1]$. Random-MiniSat was run five times on the testing set. It solved 119, 118, 119, 116 and 117 problems, which is on average a 9.2% improvement over MiniSat, compared to the 18.5% improvement achieved by NeuroComb-MiniSat. Thus, about half of the improvement in NeuroComb-MiniSat comes from the randomness introduced by the hybrid way of applying any static

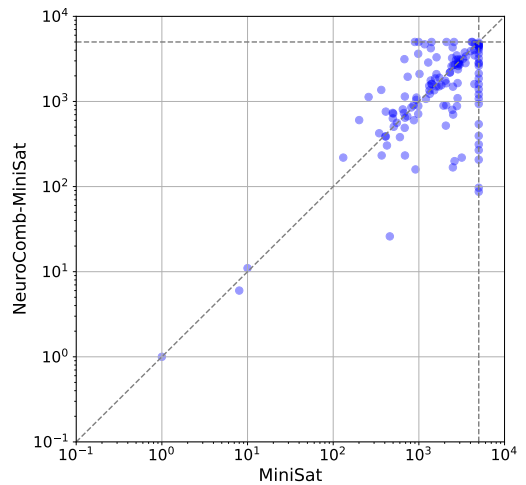


Figure 4: Time taken by NeuroComb-MiniSat and MiniSat to solve each test problem (in seconds). Each problem is represented by a dot whose location indicates the solution time of each method. The dots on the dashed lines at 5000 seconds indicate failures. MiniSat fails on many instances that NeuroComb-MiniSat solves in under 1000 seconds, demonstrating the power of the approach.

information; the other half is due to the better accuracy of this information that the GNN provides. In sum, *the high-quality predictions and the hybrid approach of applying the static information contribute about equally to the effectiveness of NeuroComb-MiniSat.*

Discussion and Future Work

The current implementation of NeuroComb has two main limitations. First, training the GNN model requires a large amount of data. Once trained, however, the model is able to generalize to new problem categories and to much larger problems, so the investment in putting together a large dataset is warranted. The current dataset will also be publicly available to benefit future research. Second, only limited hyperparameter tuning of NeuroComb-MiniSat has been done so far, and it is possible that better settings exist. A compelling direction for future work is to use search methods such as reinforcement learning or evolutionary optimization both to expand the dataset and to optimize the hyperparameters.

Conclusion

This paper proposes a machine learning approach, NeuroComb, to make CDCL SAT solving both more effective and more practical. The main idea is to train a GNN model to identify both important variables and important clauses, and use the neural predictions as static information to inform the VSIDS branching heuristic. The model inference is performed only once before the SAT solving starts and the resulting offline predictions are applied periodically during the solving. Implemented in the classic MiniSat solver, this approach made it possible to solve more instances. NeuroComb is thus a promising and practical approach to improving SAT solving efficiency through modern machine learning.

References

- Audemard, G.; and Simon, L. 2018. On the glucose SAT solver. *International Journal on Artificial Intelligence Tools*, 27(01): 1840001.
- Balyo, T.; Froleyks, N.; Heule, M. J.; Iser, M.; Järvisalo, M.; and Suda, M. 2020. Proceedings of SAT Competition 2020: Solver and Benchmark Descriptions.
- Battaglia, P. W.; Hamrick, J. B.; Bapst, V.; Sanchez-Gonzalez, A.; Zambaldi, V.; Malinowski, M.; Tacchetti, A.; Raposo, D.; Santoro, A.; Faulkner, R.; et al. 2018. Relational inductive biases, deep learning, and graph networks. *arXiv preprint arXiv:1806.01261*.
- Clevert, D.-A.; Unterthiner, T.; and Hochreiter, S. 2015. Fast and accurate deep network learning by exponential linear units (elus). *arXiv preprint arXiv:1511.07289*.
- Davis, M.; Logemann, G.; and Loveland, D. 1962. A machine program for theorem-proving. *Communications of the ACM*, 5(7): 394–397.
- Eén, N.; and Sörensson, N. 2003. An extensible SAT-solver. In *International conference on theory and applications of satisfiability testing*, 502–518. Springer.
- Fey, M.; and Lenssen, J. E. 2019. Fast graph representation learning with PyTorch Geometric. *arXiv preprint arXiv:1903.02428*.
- Fleury, A. B. K. F. M.; and Heisinger, M. 2020. CaDiCaL, Kissat, Paracooba, Plingeling and Treengeling entering the SAT Competition 2020. *SAT COMPETITION 2020*, 50.
- Gilmer, J.; Schoenholz, S. S.; Riley, P. F.; Vinyals, O.; and Dahl, G. E. 2017. Neural message passing for quantum chemistry. In *International conference on machine learning*, 1263–1272. PMLR.
- Gori, M.; Monfardini, G.; and Scarselli, F. 2005. A new model for learning in graph domains. In *Proceedings. 2005 IEEE International Joint Conference on Neural Networks, 2005.*, volume 2, 729–734. IEEE.
- Han, J. M. 2020. Enhancing SAT solvers with glue variable predictions. *arXiv preprint arXiv:2007.02559*.
- Heule, M. J.; Järvisalo, M. J.; Suda, M.; et al. 2018. Proceedings of sat competition 2018: Solver and benchmark descriptions.
- Hoos, H. H.; and Stützle, T. 2000. SATLIB: An online resource for research on SAT. *Sat*, 2000: 283–292.
- Huang, G.; Liu, Z.; Van Der Maaten, L.; and Weinberger, K. Q. 2017. Densely connected convolutional networks. In *Proceedings of the IEEE conference on computer vision and pattern recognition*, 4700–4708.
- Jackson, D. 2002. Alloy: a lightweight object modelling notation. *ACM Transactions on Software Engineering and Methodology (TOSEM)*, 11(2): 256–290.
- Janota, M.; Lynce, I.; and Marques-Silva, J. 2015. Algorithms for computing backbones of propositional formulae. *Ai Communications*, 28(2): 161–177.
- Jaszczur, S.; Łuszczczyk, M.; and Michalewski, H. 2020. Neural heuristics for SAT solving. *arXiv preprint arXiv:2005.13406*.
- Kilby, P.; Slaney, J.; Thiébaux, S.; Walsh, T.; et al. 2005. Backbones and backdoors in satisfiability. In *AAAI*, volume 5, 1368–1373.
- Kipf, T. N.; and Welling, M. 2016. Semi-supervised classification with graph convolutional networks. *arXiv preprint arXiv:1609.02907*.
- Kurin, V.; Godil, S.; Whiteson, S.; and Catanzaro, B. 2019. Improving SAT solver heuristics with graph networks and reinforcement learning.
- Kurin, V.; Godil, S.; Whiteson, S.; and Catanzaro, B. 2020. Improving SAT solver heuristics with graph networks and reinforcement learning. In *Advances in Neural Information Processing Systems*.
- Lauria, M.; Elffers, J.; Nordström, J.; and Vinyals, M. 2017. CNFgen: A generator of crafted benchmarks. In *International Conference on Theory and Applications of Satisfiability Testing*, 464–473. Springer.
- Li, G.; Muller, M.; Thabet, A.; and Ghanem, B. 2019. Deepgcns: Can gcns go as deep as cnns? In *Proceedings of the IEEE/CVF International Conference on Computer Vision*, 9267–9276.
- Li, Q.; Han, Z.; and Wu, X.-M. 2018. Deeper insights into graph convolutional networks for semi-supervised learning. In *Proceedings of the AAAI Conference on Artificial Intelligence*, volume 32.
- Liaw, A.; Wiener, M.; et al. 2002. Classification and regression by randomForest. *R news*, 2(3): 18–22.
- Loshchilov, I.; and Hutter, F. 2017. Decoupled weight decay regularization. *arXiv preprint arXiv:1711.05101*.
- Loukas, A. 2019. What graph neural networks cannot learn: depth vs width. *arXiv preprint arXiv:1907.03199*.
- Marques-Silva, J.; Lynce, I.; and Malik, S. 2021. Conflict-driven clause learning SAT solvers. In *Handbook of Satisfiability: Second Edition. Part 1/Part 2*, 133–182. IOS Press BV.
- Mesquita, D.; Souza, A.; and Kaski, S. 2020. Rethinking pooling in graph neural networks. In Larochele, H.; Ranzato, M.; Hadsell, R.; Balcan, M. F.; and Lin, H., eds., *Advances in Neural Information Processing Systems*, volume 33, 2220–2231. Curran Associates, Inc.
- Moskewicz, M. W.; Madigan, C. F.; Zhao, Y.; Zhang, L.; and Malik, S. 2001. Chaff: Engineering an Efficient SAT Solver. In *Proceedings of the 38th Annual Design Automation Conference, DAC '01*, 530–535. New York, NY, USA: Association for Computing Machinery.
- Parkes, A. J. 1997. Clustering at the phase transition. In *AAAI/IAAI*, 340–345. Citeseer.
- Paszke, A.; Gross, S.; Massa, F.; Lerer, A.; Bradbury, J.; Chanan, G.; Killeen, T.; Lin, Z.; Gimelshein, N.; Antiga, L.; et al. 2019. Pytorch: An imperative style, high-performance deep learning library. *arXiv preprint arXiv:1912.01703*.
- Previti, A.; and Järvisalo, M. 2018. A preference-based approach to backbone computation with application to argumentation. In *Proceedings of the 33rd Annual ACM Symposium on Applied Computing*, 896–902.

- Santurkar, S.; Tsipras, D.; Ilyas, A.; and Mađry, A. 2018. How does batch normalization help optimization? In *Proceedings of the 32nd international conference on neural information processing systems*, 2488–2498.
- Scarselli, F.; Gori, M.; Tsoi, A. C.; Hagenbuchner, M.; and Monfardini, G. 2008. The graph neural network model. *IEEE Transactions on Neural Networks*, 20(1): 61–80.
- Selsam, D.; and Bjørner, N. 2019. Guiding high-performance SAT solvers with unsat-core predictions. In *International Conference on Theory and Applications of Satisfiability Testing*, 336–353. Springer.
- Selsam, D.; Lamm, M.; Bünz, B.; Liang, P.; de Moura, L.; and Dill, D. L. 2018. Learning a SAT solver from single-bit supervision. *arXiv preprint arXiv:1802.03685*.
- Silva, J. P. M.; and Sakallah, K. A. 2003. GRASP—a new search algorithm for satisfiability. In *The Best of ICCAD*, 73–89. Springer.
- Wojtowysch, S.; and E, W. 2020. Can Shallow Neural Networks Beat the Curse of Dimensionality? A Mean Field Training Perspective. *IEEE Transactions on Artificial Intelligence*, 1(2): 121–129.
- Wu, Z.; Pan, S.; Chen, F.; Long, G.; Zhang, C.; and Philip, S. Y. 2020. A comprehensive survey on graph neural networks. *IEEE transactions on neural networks and learning systems*, 32(1): 4–24.
- Yolcu, E.; and Póczos, B. 2019. Learning local search heuristics for boolean satisfiability. In *Advances in Neural Information Processing Systems*, 7992–8003.
- Zhou, J.; Cui, G.; Hu, S.; Zhang, Z.; Yang, C.; Liu, Z.; Wang, L.; Li, C.; and Sun, M. 2020. Graph neural networks: A review of methods and applications. *AI Open*, 1: 57–81.